

Tensile and fatigue crack growth properties of high strength stainless steel with high resistance to hydrogen embrittlement in 100 MPa hydrogen gas

Akihiro ORITA^{1,a}, Takashi MATSUO^{2,b},
Saburo MATSUOKA^{3,4,c} and Yukitaka MURAKAMI^{3,4,d}

¹ Department of Hydrogen Energy Systems, Graduate School of Engineering, Kyushu University,
Moto-oka, Nishi-ku, Fukuoka, 819-0395, Japan

² Hydrogen Energy Test and Research Center (HyTReC),
915-1, Tomi, Itoshima-City, Fukuoka, 819-1133, Japan

³ The Research Center for Hydrogen Industrial Use and Storage (HYDROGENIUS),
National Institute of Advanced Industrial Science and Technology (AIST),
Moto-oka, Nishi-ku, Fukuoka, 819-0395, Japan

⁴ International Institute for Carbon Neutral Energy Research (WPI-I²CNER), Kyushu University,
744 Moto-oka, Nishi-ku, Fukuoka 819-0395, Japan

^a 3TE10092G@kyushu-u.ac.jp, ^b tmatsu@hytrec.jp,

^c saburo.matsuoka.121@m.kyushu-u.ac.jp, ^d murakami.yukitaka.600@m.kyushu-u.ac.jp

Keywords: hydrogen embrittlement, austenitic stainless steel, fatigue crack growth properties, tensile properties

Abstract

The sensitivity of high strength austenitic stainless steel HP160 to hydrogen was investigated by conducting tensile tests and fatigue crack growth tests in hydrogen gas with a pressure of about 100 MPa. Tests for Type316L and Type304 austenitic stainless steels were also carried out to compare with HP160. The tensile strength was 919 MPa for HP160, 561 MPa for Type316L and 715 MPa for Type304. Type316L (12.1 mass %Ni) is a stable austenitic stainless steel, and Type304 (8.07 mass %Ni) is a meta-stable austenitic stainless steel. HP160 has 9.71 mass % Ni and small amounts of N, Mn, Nb, Mo and Cu. For Type304, the tensile strength (σ_B) and reduction of area (ϕ) in hydrogen gas were much lower than those in air. In contrast, decrease in σ_B and ϕ in hydrogen gas of Type316L was small. HP160 also showed only a slight decrease in σ_B and ϕ in hydrogen gas, regardless of low content of Ni, 9.71 mass %. The fatigue crack growth rate (da/dN) for Type304 was more than 10 times faster in hydrogen gas than that in air, while the acceleration of da/dN in hydrogen gas for HP160 and Type316L was very small. It is presumed that a small addition of nitrogen increased the strength properties and stabilized the austenitic phase of HP160 resulting in high strength and high resistance against hydrogen embrittlement.

1. Introduction

A 70 MPa fuel cell vehicle and 70 MPa hydrogen station is scheduled to be commercialized in 2015 in Japan. Although Type316L has high hydrogen embrittlement (HE) property, the strength is not sufficiently high for use of 70 MPa fuel cell vehicle (FCV) and hydrogen station. It is known that the addition of nitrogen to austenitic stainless steels stabilizes the austenitic phase [1] and

increases the tensile strength [2]. In addition, it is reported that the stabilization of the austenitic phase due to the nitrogen addition improves the resistance to HE [3,4].

In this study, tensile tests and fatigue crack growth test in 100 MPa hydrogen gas were conducted for a high-strength austenitic stainless steel HP160[5] with small addition of nitrogen (N). Type316L and Type304 were also tested in 78 MPa - 115 MPa hydrogen gas as the reference. Comparing the tensile properties and fatigue crack growth properties of three austenitic stainless steels, it is revealed that HP160 shows the high static and fatigue strength as well as high resistance against HE.

2. Experimental

Table 1 shows the chemical composition and Vickers hardness of HP160, Type316L and Type 304. Comparing with Type 304, N, Mn, Nb, Mo and Cu are added to HP160. The stability of austenite can be judged by M_{d30} , which is defined as the temperature at which 50% of the austenite transforms into martensite by applying true strain of 0.3 to single-phase austenite specimen. The value of M_{d30} estimated by the formula proposed by Angle [1] was -4.5°C for Type316L and 43.1°C for Type 304. Therefore, Type316L is a stable austenitic stainless steel, and Type304 is a meta-stable austenitic stainless steel. M_{d30} of HP160 was -235.8°C . Thus, HP160 has a very stable austenite phase compared to Type316L and Type 304.

Tensile specimens and CT specimens were machined from a 105 mm diameter round bar according to ASTM E 142 and G 647, respectively. The specimen dimensions are shown in Fig.1. The axis of tensile specimens is parallel to the rolling direction of the round bar. The direction of fatigue crack growth in CT specimens is perpendicular to the rolling direction.

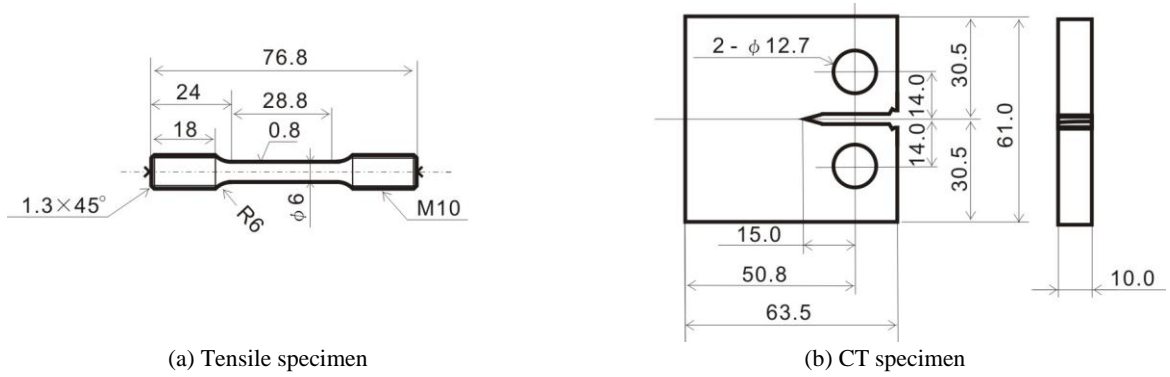
Tensile tests were conducted in air and 78-115 MPa hydrogen gas at room temperature, using a hydraulic servo testing machine with a high pressure vessel. The strain rate of tensile tests was $6.94 \times 10^{-5} \text{ s}^{-1}$.

Fatigue crack growth tests were conducted in air and 100-115 MPa hydrogen gas at room temperature, using a hydraulic servo testing machine with a high pressure vessel. ΔP -constant ΔK -increasing fatigue tests were conducted at a stress ratio of $R = 0.1$ and test frequency of $f = 1 \text{ Hz}$ to obtain the fatigue crack growth curve, da/dN versus ΔK . Here, da/dN is the crack growth rate, ΔK is the stress intensity factor range, and ΔP is the load range. In addition, ΔK -constant fatigue tests were conducted at $R = 0.1$ and $f = 0.01, 0.1, 1$ and 5 Hz to investigate the frequency dependency of the fatigue crack growth rate.

The microstructure near the fatigue crack was investigated by EBSD. The fracture surfaces of tensile specimens and fatigue specimens were observed by SEM.

Table 1. Chemical composition [mass %], Vickers hardness HV and M_{d30} [$^{\circ}\text{C}$]

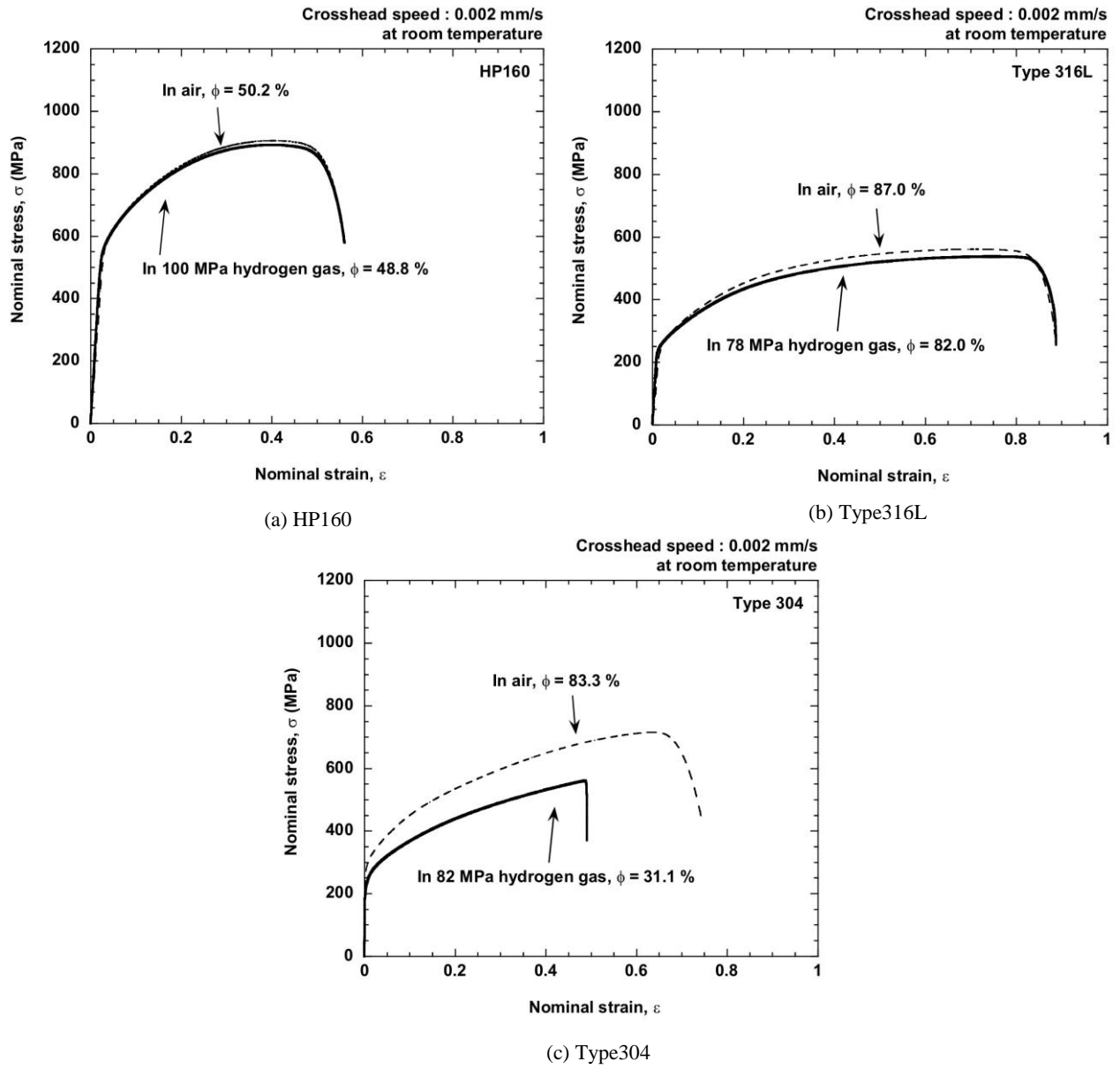
	C	Si	Mn	P	S	Cr	Mo	Ni	Nb	N	Cu	HV	M_{d30}
HP160	0.03	0.47	3.98	0.016	0.0015	20.7	2.29	9.71	0.28	0.39	0.11	238	-235.8
Type 316L	0.023	0.54	0.86	0.022	0.001	17.61	2.1	12.09	-	-	-	148	-4.5
Type 304	0.06	0.43	0.84	0.028	0.002	18.22	0.28	8.07	-	-	-	174	43.1



(a) Tensile specimen

(b) CT specimen

Fig.1. Dimensions of tensile specimen and CT specimen



(a) HP160

(b) Type316L

(c) Type304

Fig.2. Nominal stress and strain curves of HP160, Type316L and Type 304 in high-pressure hydrogen gas and air.

3. Results and Discussion

3.1 Tensile properties in 78 MPa - 100 MPa hydrogen gas

Figure 2 shows the nominal stress and strain curves in hydrogen gas and air for HP160, Type316L and Type 304. In HP160 and Type316L, no definite difference between hydrogen gas and air were observed in 0.2% proof strength ($\sigma_{0.2}$), tensile strength (σ_B), elongation (δ) and reduction of area (ϕ). However, the strength properties of HP160 were much higher than those of Type316L. For example, $\sigma_B = 892$ MPa for HP160, and $\sigma_B = 537$ MPa for Type316L. In Type 304, not only δ and ϕ but also $\sigma_{0.2}$ and σ_B were lower in 82 MPa hydrogen gas than in air.

Figure 3 shows the tensile fracture morphologies of HP160, Type316L and Type 304 obtained in high-pressure hydrogen gas. A typical cup-and-cone fracture occurred for HP160 in 100 MPa hydrogen gas ((a) and (b)) and for Type316L in 78 MPa hydrogen gas ((d) and (e)). The fracture surfaces of HP160 and Type316L were covered with dimples ((c) and (f)). In contrast, Type 304 did not show the cup-and-cone fracture in 82 MPa hydrogen gas ((g) and (h)). The fracture surface was relatively flat, and the fracture surface was less ductile ((i)).

The content of Ni is an important parameter for HE in tensile fracture for austenitic stainless steels[6]. It is known that decrease in σ_B and ϕ in 35 MPa hydrogen gas of Type316 and Type316L with the Ni content higher than 12 mass % is small, because of stable austenitic phase [6]. On the other hand, meta-stable austenitic stainless steel, Type304 with about 8 mass % Ni, shows large decrease in σ_B and ϕ in high-pressure hydrogen gas [6]. In this study, as shown in Fig.2, decrease in σ_B and ϕ in hydrogen gas of Type316L (12.1 mass % Ni) is small, on the other hand, Type304 (8.07 mass % Ni) shows large decrease in σ_B and ϕ in hydrogen gas as reported in [6]. HP160 shows no definite difference in σ_B and ϕ between 100 MPa hydrogen gas and air, regardless of low Ni content,

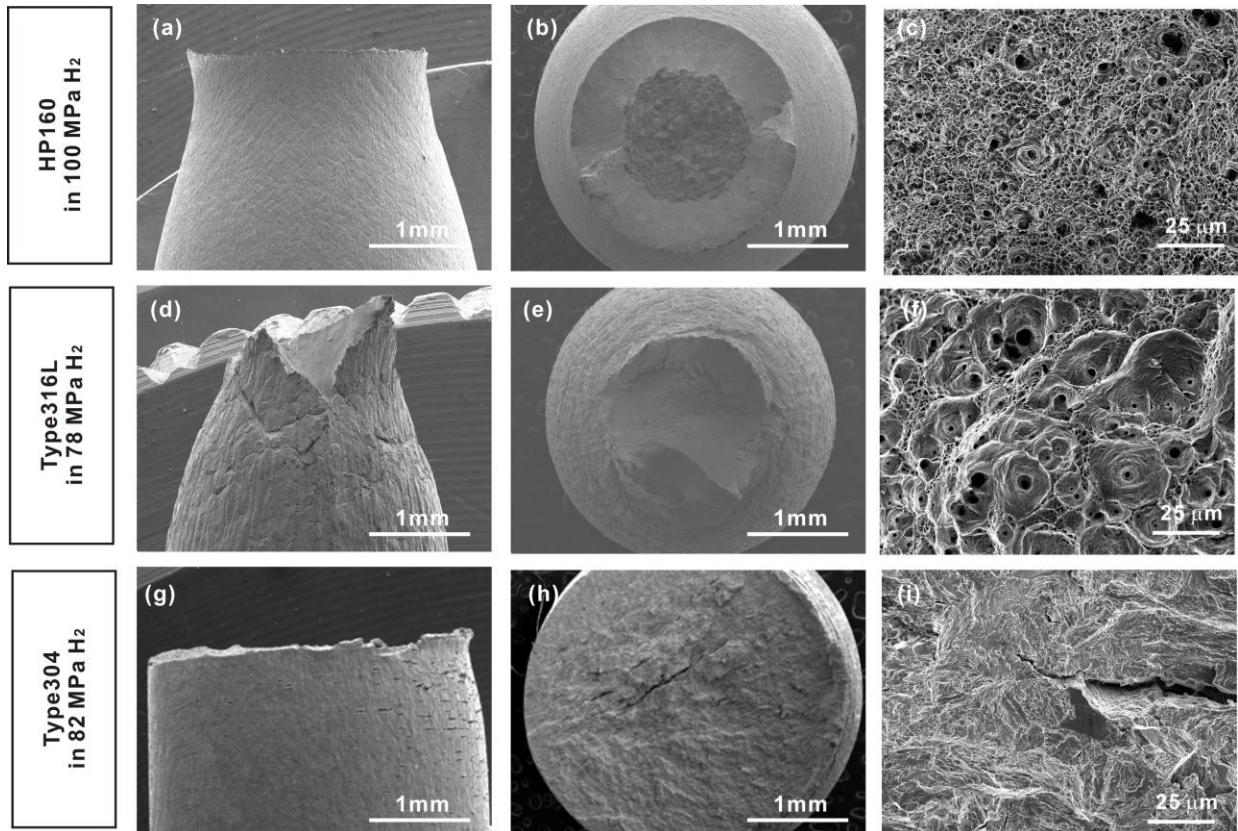


Fig. 3. Tensile fracture morphologies of HP160, Type316L and Type 304 in high pressure hydrogen gas.
Strain rate : $6.94 \times 10^{-5} \text{ s}^{-1}$

9.71 mass %. This is because addition of N not only increases the strength properties[2], but also stabilizes the austenitic phase[1]. Accordingly, it can be concluded from the results of tensile tests that HP160 shows the high strength as well as the high resistance against HE.

3.2 Fatigue crack growth properties in 100 MPa or 115 MPa hydrogen gas

Figures 4 and 5 show the fatigue crack growth properties at $R = 0.1$ and $f = 1$ Hz. Figure 4 shows that the fatigue crack growth curve, da/dN versus ΔK , for Type 304 in 115 MPa hydrogen gas is much higher than that in air. However, the fatigue crack growth curves for HP160 in 100 MPa hydrogen gas and for Type316L in 115 MPa hydrogen gas are only slightly higher than those in air. Figure 5 shows that the relative crack growth rate, $(da/dN)_{H_2}/(da/dN)_{air}$ in terms of test frequency, f . Figure 5 shows that the crack growth rate is hardly accelerated for HP160 in hydrogen gas. As shown in Fig.4, the fatigue crack growth rate in air for HP160 is much lower than that for Type316L and Type 304 in air. It can be understood that the lower crack growth rate for HP160 is due to the crack closure from Fig.6 which shows the relationship between load and differential COD. The differential COD is calculated by the unloading elastic compliance method. This figure shows that the strong crack closure occurred in HP160 in 100 MPa hydrogen gas and air.

Figure 7 shows the correlation between the crack growth rate, da/dN , and the effective stress intensity factor range, ΔK_{eff} , for HP160, Type316L and Type304. $da/dN-\Delta K_{eff}$ curves for HP160 and Type316L are slightly higher in hydrogen gas than in air, while $da/dN-\Delta K_{eff}$ curves for Type304 is much higher in hydrogen gas.

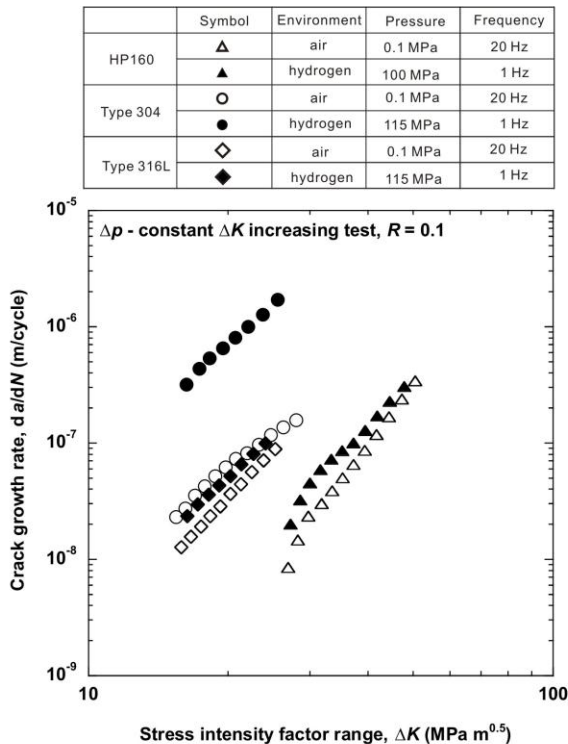


Fig.4. Relationship between crack growth rate and stress intensity factor range of HP160, Type316L and Type 304.

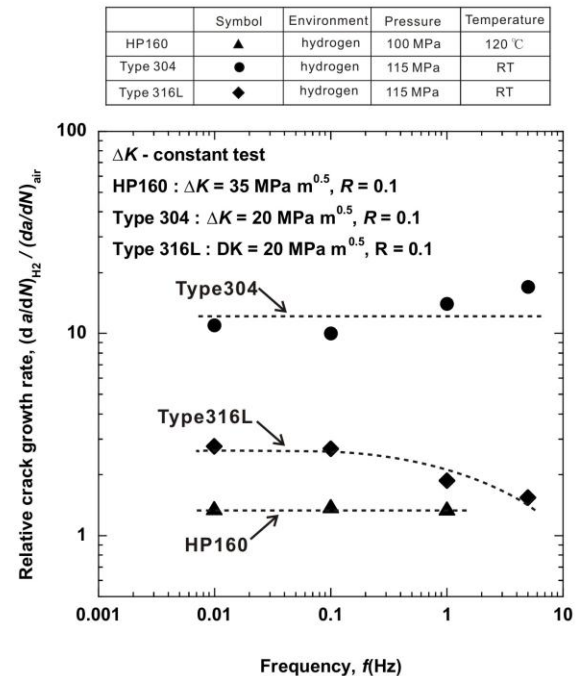


Fig.5. Relationship between relative crack growth rate and frequency of HP160, Type316L and Type 304.

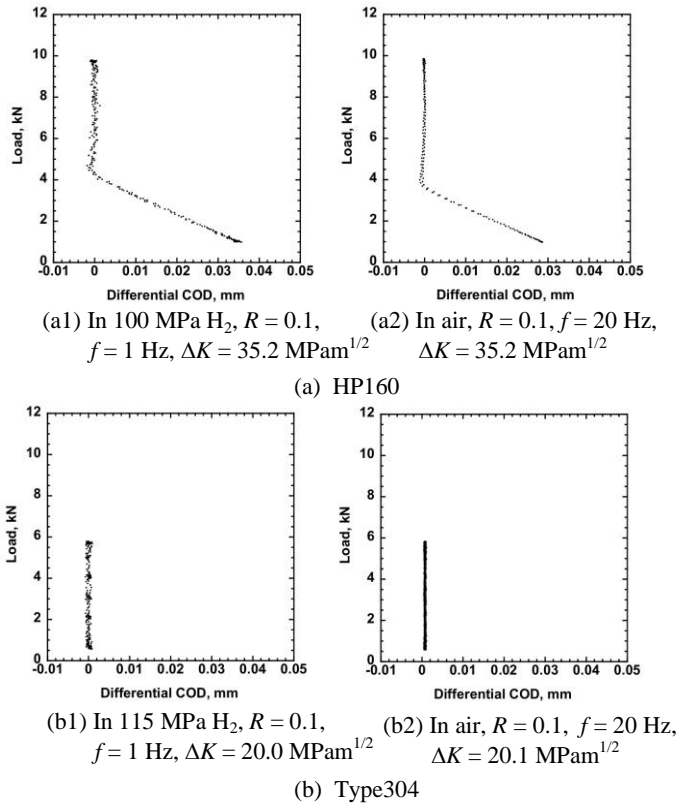


Fig.6. Relationship between load and differential COD of HP160 and Type304.

	Symbol	Environment	Pressure	Frequency
HP160	△	air	0.1 MPa	20 Hz
	▲	hydrogen	100 MPa	1 Hz
Type 304	○	air	0.1 MPa	20 Hz
	●	hydrogen	115 MPa	1 Hz
Type 316L	◇	air	0.1 MPa	20 Hz
	◆	hydrogen	115 MPa	1 Hz

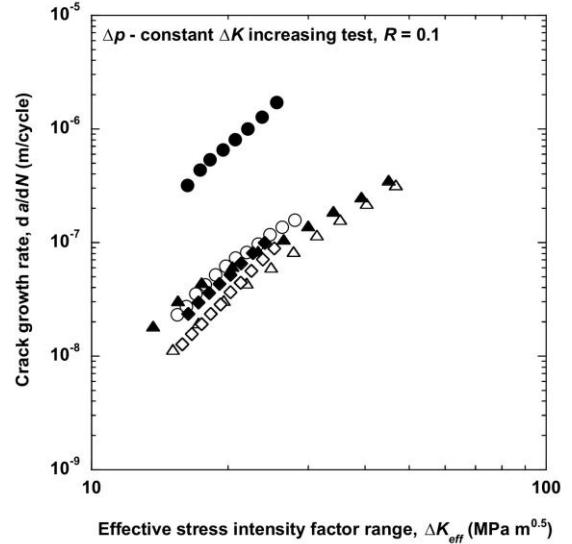


Fig.7. Relationship between crack growth rate and effective stress intensity factor range of HP160, Type316L and Type304.

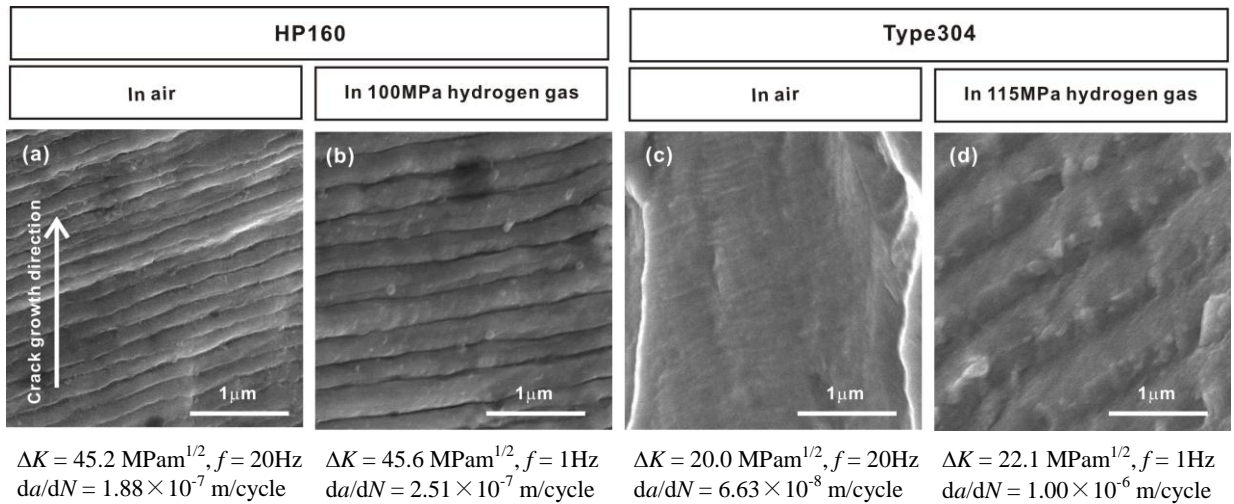


Fig.8. Striations of HP160, Type316L and Type 304 in high-pressure hydrogen gas and air.

Figure 8 shows SEM images of the striations observed in the specimens exposed to air or high-pressure hydrogen gas. In HP160, ductile striations were observed in both air (Fig. 8(a)) and 100 MPa hydrogen gas (Fig. 8(b)). Ductile striations were also formed for Type316L in 115 MPa hydrogen gas and air. In contrast, in Type 304, ductile striations were observed in air (Fig. 8(c)), and flat and widely spaced striations were observed in 115 MPa hydrogen gas (Fig. 8(d)). According to the mechanism proposed by Murakami et al. [7] and Matsuoka et al. [8], the flat and wide striations due to hydrogen are caused by hydrogen concentration and slip localization at fatigue crack tip.

Murakami et al. [9] visualized hydrogen induced slip localization at the fatigue crack tip by EBSD analysis of austenitic stainless steels Types 304 and 316L.

Figure 9 shows the results of EBSD analysis of HP160, Type316L and Type 304 near the tips of fatigue cracks. As reported by Murakami et al. [9], α phase (red color in Fig.9) was observed near cracks in Type 304 (Fig. 9(e) and (f)). The α phase is strain-induced martensite, which was induced by plastic deformation. The strain-induced martensite zones near cracks were smaller in the hydrogen gas than in air. For HP160 and Type316L, on the other hand, the strain-induced martensite zones were hardly observed in hydrogen gas and air in this magnifications. This is because the austenitic phase is stable for HP160 and Type316L. The stabilization of austenitic phase for HP160 is due to the addition of a small amount of N.

It can be concluded from the above results of tensile tests and fatigue crack growth tests showed that HP160 is the high-strength austenitic stainless steel with the high resistance against HE.

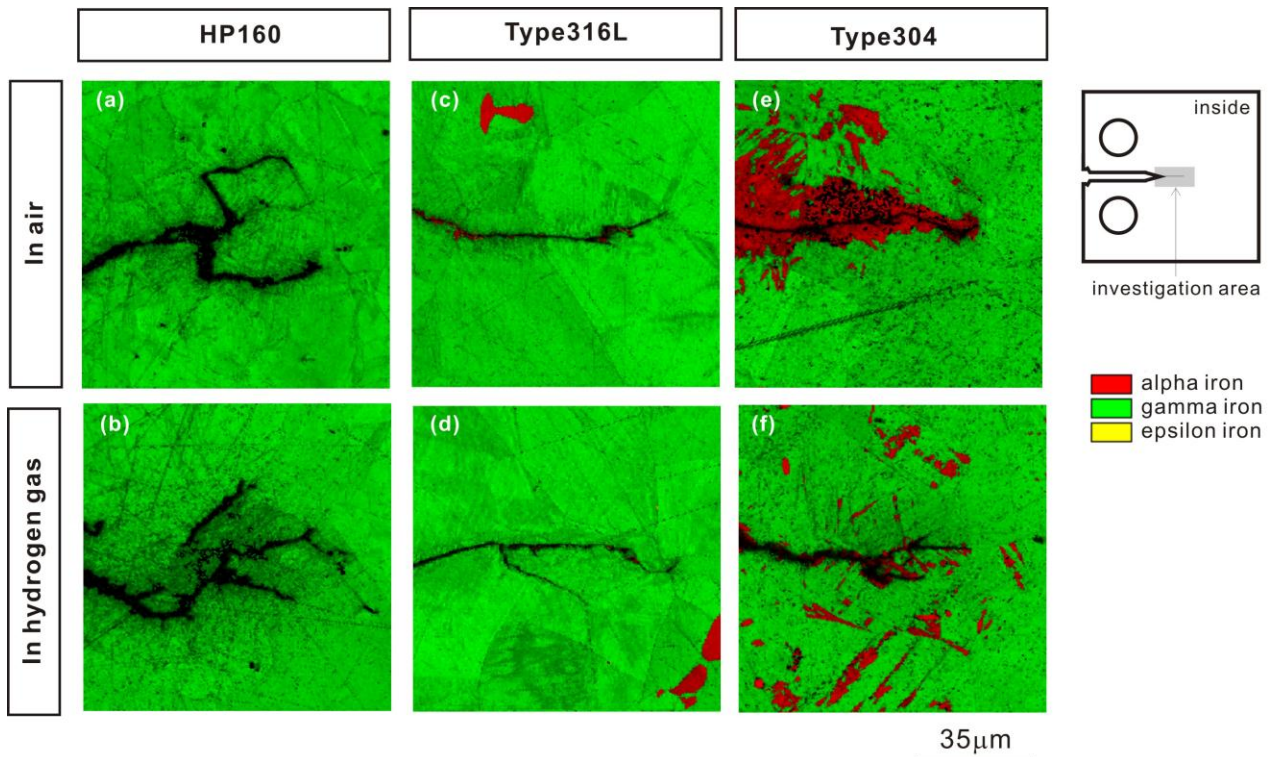


Fig.9. Phase maps on image quality maps of HP160 (a,b), Type316L (c,d) and Type 304 (e,f).

- (a) HP160, in air : $\Delta K=53.0 \text{ MPa m}^{1/2}$, $R = 0.1$, $f = 20 \text{ Hz}$, $da/dN = 4.46 \times 10^{-7} \text{ m/cycle}$ (at the crack tip)
- (b) HP160, in 100MPa H_2 : $\Delta K=50.0 \text{ MPa m}^{1/2}$, $R = 0.1$, $f = 1 \text{ Hz}$, $da/dN = 3.82 \times 10^{-7} \text{ m/cycle}$ (at the crack tip)
- (c) Type316L, in air : $\Delta K=25.3 \text{ MPa m}^{1/2}$, $R = 0.1$, $f = 20 \text{ Hz}$, $da/dN = 8.84 \times 10^{-8} \text{ m/cycle}$ (at the crack tip)
- (d) Type316L, in 115MPa H_2 : $\Delta K=24.6 \text{ MPa m}^{1/2}$, $R = 0.1$, $f = 1 \text{ Hz}$, $da/dN = 1.07 \times 10^{-7} \text{ m/cycle}$ (at the crack tip)
- (e) Type304, in air : $\Delta K=29.5 \text{ MPa m}^{1/2}$, $R = 0.1$, $f = 20 \text{ Hz}$, $da/dN = 1.70 \times 10^{-7} \text{ m/cycle}$ (at the crack tip)
- (f) Type304, in 115MPa H_2 : $\Delta K=29.5 \text{ MPa m}^{1/2}$, $R = 0.1$, $f = 1 \text{ Hz}$, $da/dN = 2.60 \times 10^{-6} \text{ m/cycle}$ (at the crack tip)

4. Conclusions

The sensitivity of high strength austenitic stainless steel HP160 to hydrogen was investigated by conducting tensile and fatigue crack growth tests of HP160, Type316L and Type 304 in hydrogen gas with pressure of 78 MPa - 115 MPa. Type316L (12.1 mass %Ni) is a stable austenitic stainless steel, and Type304 (8.07 mass %Ni) is a meta-stable austenitic stainless steel. HP160 has small amounts of N, Mn, Nb, Mo and Cu added to Type304. The conclusions can be summarized as follows.

1. The tensile strength and reduction of area (ϕ) for HP160 and Type316L were slightly lower in hydrogen gas than in air. On the other hand, σ_B and ϕ of Type 304 in hydrogen gas were much lower than that in air.
2. HP160 and Type316L showed cup-and-cone fracture in the air and hydrogen gas. Dimples were formed on the fracture surfaces. In contrast, Type 304 did not show cup-and-cone fracture in hydrogen gas. The fracture surface was less ductile.
3. The fatigue crack growth rate in HP160 and Type316L was hardly accelerated in high-pressure hydrogen gas. In contrast, the fatigue crack growth rate in Type 304 was more than 10 times faster in hydrogen gas than in air.
4. Ductile striations were formed on the fatigue crack surfaces of HP160 and Type316L in both hydrogen gas and air. For Type 304, ductile striations were formed in air. On the other hand, flat and widely spaced striations were formed in hydrogen gas.
5. Nitrogen addition contributes to the increase in strength properties and stabilization of austenitic phase and eventually high resistance against hydrogen embrittlement of HP160.

Acknowledgments

This research is supported by the NEDO Fundamental Research Project on Advanced Hydrogen Science (2006 to 2012). The authors gratefully acknowledge the support of the International Institute for Carbon-Neutral Energy Research (WPI-I2CNER), sponsored by the Japanese Ministry of Education, Culture, Sport, Science and Technology. The authors acknowledge Iwatani Corporation for preparing the specimens and discussions.

Reference

- [1] T. Angel: Journal of the Iron and Steel Institute 177 (1954), p.165
- [2] M. Byrnes, M. Grujicic and W. Owen: Acta Metallurgica 35 (7) (1987), p.1853
- [3] A. Onizawa, M. Islam, M. Ojima and Y. Tomota: ARPN Journal of Engineering and Applied Sciences Vol.1 (2006), p.12
- [4] P. Rozenak: Journal of Materials Science 25 (5) (1990), p.2532
- [5] P. Koerner, W. Hiller, R. Wink, H. Strackerjahn and M. Goeken: ASME Conference Proceedings (2004), p.1
- [6] C. San Marchi, T. Michler, K. Nibur, B. Somerday : International Journal of Hydrogen Energy 35 (18) (2010), p. 9736.
- [7] Y. Murakami, T. Kanezaki, Y. Mine, S. Matsuoka: Hydrogen embrittlement mechanism in fatigue of austenitic stainless steels, Metallurgical and Materials Transactions A 39 (6) (2008), p.1327
- [8] S. Matsuoka, N. Tsutsumi, Y. Murakami: The Japan Society of Mechanical Engineers, A (2008) p.1528 (Japanese)
- [9] Y. Murakami, T. Kanezaki, Y. Mine: Metallurgical and Materials Transactions A 41 (10) (2010) p.2548